MOLECULAR AND CELLULAR BIOLOGY, Feb. 2006, p. 940–954 Vol. 26, No. 3
0270-7306/06/$08.00+0 doi:10.1128/MCB.26.3.940–954.2006

Accelerated Ovarian Failure Induced by 4-Vinyl Cyclohexene Diepoxide in Nrf2 Null Mice

Xiaoming Hu,[1]† Jenny R. Roberts,[2] Patrick L. Apopa,[1,3] Yuet Wai Kan,[4] and Qiang Ma[1]*

Receptor Biology Laboratory, Toxicology and Molecular Biology Branch,[1] and Pathology and Physiology Research Branch,[2] Health Effects Laboratory Division, National Institute for Occupational Safety and Health, Centers for Disease Control and Prevention, and Department of Biochemistry and Molecular Pharmacology, West Virginia University,[3] Morgantown, West Virginia, and Department of Laboratory Medicine and Howard Hughes Medical Institute, University of California, San Francisco, California[4]

Received 27 May 2005/Returned for modification 22 July 2005/Accepted 11 November 2005

Genetic and biochemical analyses have uncovered an essential role for nuclear factor erythroid 2-related factor 2 (Nrf2) in regulating phase II xenobiotic metabolism and antioxidant response. Here we show that Nrf2 protects against the ovarian toxicity of 4-vinylcyclohexene diepoxide (VCD) in mice. Nrf2$^{-/-}$ female mice exposed to VCD exhibit an age-dependent decline in reproduction leading to secondary infertility accompanied by hypergonadotropic hypogonadism after 30 weeks of age. VCD is shown to selectively destroy small ovarian follicles, resulting in early depletion of functional follicles. Treatment with VCD induces apoptotic death in cultured cells and in ovarian follicles, suggesting apoptosis as a mechanism of follicle loss. Loss of Nrf2 function blocks the basal and inducible expression of microsomal epoxide hydrolase, a key enzyme in the detoxification of VCD, and increases the oxidative stress in cells that is further exacerbated by VCD. Foxo3a, a repressor in the early stages of follicle activation, displays reduced expression in Nrf2$^{-/-}$ ovaries, causing accelerated growth of follicles in the absence of exposure to exogenous chemicals. Furthermore, Foxo3a is degraded through the 26S proteasome pathway in untreated cells and is induced by VCD via both Nrf2-dependent transcription and protein stabilization. This study demonstrates that Nrf2 serves as an essential sensor and regulator of chemical homeostasis in ovarian cells, protecting the cells from toxic chemicals by controlling metabolic detoxification, reactive oxygen species defense, and Foxo3a expression. In addition, these findings raise the possibility that exposure to environmental or occupational ovotoxicants plays a role in the premature ovarian failure commonly associated with infertility and premature aging in women.

Cells cope with toxic chemicals by eliciting adaptive responses that result in elimination of the toxicants, reduction of toxic responses, and repair of tissue damage, thereby maintaining chemical homeostasis and physiological functions (30). Many adaptive responses are controlled by chemical-activated receptor or transcription factors, which sense changes in the chemical environment of cells, by themselves or with associated proteins, and coordinately regulate multiple transcriptional responses to combat toxic insults and tissue lesions (30, 43). Nrf2 (nuclear factor erythroid 2-related factor 2) is a member of the CNC-bZip (cap 'n' collar basic leucine zipper) subfamily of leucine zipper transcription factors. Evidence accumulated in recent years suggests that Nrf2 and its cytoplasmic binding protein, Keap1, constitute one of the chemical-sensing and transcription systems that play an essential role(s) in cellular protection against a range of chemical toxicity, carcinogenesis, and pathological processes (10, 21, 34, 36).

Several features of the mode of action of Nrf2/Keap1 are noteworthy. First, Nrf2 controls both the constitutive and inducible expression of a spectrum of protective genes, implicating Nrf2 in the maintenance of chemical homeostasis under both physiological and chemical-challenged conditions. Second, transcription by Nrf2 is governed by AREs (antioxidant response elements) located in the enhancers of two sets of target genes: phase II detoxification enzymes such as glutathione *S*-transferase 1A and NAD(P)H:quinone oxidoreductase (NQO1) and antioxidant enzymes such as glutathione synthetase and γ-glutamylcysteine synthetase (6, 20, 29, 36). Phase II enzymes detoxify chemicals through reduction and conjugation reactions, whereas antioxidant enzymes are directly involved in protection against reactive oxygen species (ROS). Third, inducers of Nrf2 target genes consist of a wide range of chemicals with diverse structures. Recent evidence suggests a mode of activation of Nrf2 in which chemical signals modify the thiol groups of Keap1, leading to dissociation of Nrf2 from Keap1, followed by translocation of Nrf2 into the nucleus (10). Fourth, the CNC-bZip proteins (NF-E2, Nrf1, Nrf2, and Nrf3) are highly homologous in the DNA-binding region, suggesting overlapping functions among CNC-bZip proteins in the transcription of target genes. Indeed, targeted knockout (KO) of Nrf1 and Nrf2 in mice revealed that the two proteins partially compensate for each other in hepatic detoxification of oxidative insults (26). Lastly, Nrf2 null mice are viable and can mature to give birth. However, these mice develop lupus-like autoimmune dysfunction in the absence of apparent exposure to toxic chemicals, implying a physiological role for Nrf2 in autoimmune regulation (28, 44).

* Corresponding author. Mailing address: Receptor Biology Laboratory, TMBB/HELD/NIOSH/CDC, Mailstop 3014, 1095 Willowdale Rd., Morgantown, WV 26505. Phone: (304) 285-6241. Fax: (304) 285-5708. E-mail: qam1@cdc.gov.

† Present address: Abbott Laboratories, Abbott Park, IL 60064-6122.

Mammalian females are born with a finite number of primordial follicles in the ovary, each containing an oocyte arrested in the first meiotic division and a layer of granulosa cells (38). Follicular growth, which is characterized by oocyte growth and transition of squamous to cuboidal granulosa cells, is irreversible. Follicles recruited to the growing pool undergo atresia (apoptosis) if not selected for further growth and maturation (11). Activation of resting follicles occurs through an unknown triggering mechanism(s) intrinsic to the ovary and independent of pituitary gonadotropins. Depletion of ovarian follicles through atresia during aging causes ovarian failure (i.e., menopause in women) (11). Infertility secondary to early follicular depletion in females before the age of 40 results in premature ovarian failure (POF) (1).

A limited number of genetic and environmental factors have been associated with follicle destruction and early depletion, giving rise to POF (1, 18, 32). For example, smoking is known to be associated with early menopause, and polycyclic aromatic hydrocarbons, major toxic components of cigarette smoke, cause follicle destruction in experimental animals (31). Exposure to 2-bromopropane at the work place is linked to an increase in the incidence of early menopause and infertility in female workers; the chemical is selectively toxic to ovarian follicles in animal models (23, 45). Thus, identifying genetic and environmental factors, as well as gene-environment interactions, that contribute to follicular destruction and POF is a particular health concern of women at work and in general populations.

4-Vinylcyclohexene (VCH) is an occupational ovarian toxicant produced from the dimerization of 1,3-butadiene during the manufacture of synthetic rubber, flame retardants, insecticides, and plasticizers (2). VCH is metabolized to VCH diepoxide (VCD) through cytochrome P450-catalyzed epoxidation. In rodents, VCH and VCD have been shown to damage small follicles and cause ovarian cancer (2, 17). Three lines of observation suggest that VCD is the ovotoxic form of its parent compound: (i) VCD is about 10-fold more potent than VCH in destroying follicles; (ii) mice are more sensitive than rats to VCH ovotoxicity, and the differential sensitivity correlates with the difference in the metabolic abilities of the two species to convert VCH to VCD; and (iii) the differential sensitivity to ovotoxicity in mice and rats is largely reduced when VCD is injected into the animals (39, 40). The functional impact of VCH or VCD ovotoxicity on reproduction has not been investigated.

VCD is further metabolized in the liver to less toxic metabolites through phase II reactions, among which hydration of the epoxide to a tetrio by microsomal epoxide hydrolase (mEH) is a critical step of VCD detoxification (17, 22). In light of the critical role of Nrf2 in the regulation of phase II gene expression, we postulated that Nrf2 plays certain roles in the protection against VCD ovotoxicity. The hypothesis is tested by using Nrf2 KO mice. While VCD selectively destroys primordial and primary follicles by 50% in wild-type (Wt) mice, it depletes small follicles by 95% in Nrf2 null mice, leading to POF by 30 weeks of age compared with ~50 weeks for the control. Mechanistic analyses demonstrated that depletion of follicles correlates with diminished expression of mEH in the liver and Foxo3a in the ovary, as well as increased oxidative stress and apoptosis in Nrf2 null mice. Furthermore, a synergistic action between VCD and Nrf2 null function is observed in promoting oxidative stress. Our findings suggest that Nrf2 is required for detoxification of VCD, expression of Foxo3a, and defense against oxidative stress in the ovary, which are essential for protection against VCD ovotoxicity.

MATERIALS AND METHODS

Materials. VCD (purity, >99%), sesame oil, and other chemicals were purchased from Sigma Chemical Co. (St. Louis, MO). Polyclonal antibodies specific for mouse Foxo3a (anti-FKHRL1) were obtained from Upstate (Charlottesville, VA). Reagents for immunofluorescent staining, the terminal deoxynucleotidyl-transferase-mediated dUTP-biotin nick end-labeling (TUNEL) assay, and serum hormone quantification are described in the corresponding method sections.

Animal treatment and tissue collection. Nrf2 null mice, in which the Nrf2 gene is disrupted and rendered nonfunctional by targeted gene KO, were described previously (7). The mice were rederived at the Jackson Laboratory to ensure that they were free of specific pathogens and were maintained at the NIOSH (National Institute for Occupational Safety and Health) animal care facility (29). The KO mice, with a mixed background of 129SVJ and C57BL/6, were backcrossed with C57BL/6 mice to change to a C57BL/6 genetic background (>97%). Female C57BL/6 mice (Wt) at an age of 21 days were obtained from Charles River Laboratories (Wilmington, MA) and maintained in the animal care facility for 1 week prior to treatment. Female Wt and Nrf2$^{-/-}$ mice at an age of 28 days were weight matched and dosed daily with VCD (0.57 mmol/kg of body weight/day, given intraperitoneally [i.p.]) or sesame oil (vehicle control, given i.p.) for 15 days; the dosage, route of administration, and dosing time course were based on previous studies (3, 19). Four hours after the final dosing, the mice were euthanized by CO_2 inhalation. The liver and ovaries were excised and processed for RNA, protein, and histological analyses.

Continuous-breeding assay. The continuous-breeding assay is aimed at evaluating the reproductive fitness of female mice. Wt or Nrf2$^{-/-}$ female mice at 28 days of age were treated with VCD or sesame oil once daily for 15 days as described above. The mice were then paired with healthy Wt C57BL/6 male mice for breeding starting at an age of 6 weeks. Mating pairs were placed in separate cages and inspected each morning. After a litter was weaned, the female was paired with a new male to avoid low reproducibility due to male reproductive dysfunction. When no litter was produced, the female was paired one more time with a healthy male to ensure that female infertility was reached. Litter size and cumulative number of progenies per female were recorded for each group and used to evaluate the reproductive fitness of female mice.

Histology and follicle counting. Four hours after administration of the final dose of VCD, mice were euthanized and ovaries were collected. Ovaries were trimmed of fat tissues, fixed in Bouin's solution for 24 h, embedded, serially sectioned at a thickness of 7 μm, and stained with hematoxylin and eosin (H&E) at the NIOSH Pathology Core. Developmental stages of follicles were defined as described previously (9). The numbers of oocyte-containing follicles at each developmental stage were determined in every 10th section of an ovary under a microscope as described by Borman et al. (3). The total numbers of primordial, primary, and preantral or antral follicles present in marked sections were multiplied by 10 to obtain an estimate of the total number of follicles per ovary (12, 40).

To evaluate physiological follicle development in the absence of Nrf2, ovaries were harvested from Nrf2$^{-/-}$ and C57BL/6 Wt mice on postnatal days (PND) 3, 8, 15, and 53. Ovaries were sectioned and stained with H&E. Numbers of oocyte-containing follicles at each developmental stage were counted in every 5th section for those that had been taken from PND 3, 8, or 15 mice and in every 10th section for those that had been taken from PND 53 mice. To obtain an estimate of the total number of follicles per ovary, the total number of primordial, primary, and preantral or antral follicles present in the marked section were multiplied by 5 or 10 to account for every 5th or 10th section being used in the analysis (12, 40). All ovaries were coded prior to histological analysis to ensure that all morphological and quantitative evaluation was conducted without the knowledge of genotypes.

Measurement of serum hormone levels. Blood was collected from the mouse tail as described by Hoff (15) at the indicated time points after treatment. Serum was prepared and stored at −20°C until use. Plasma follicle-stimulating hormone (FSH) and luteinizing hormone (LH) levels were measured with a competitive enzyme immunoassay kit from Amersham Biosciences (Piscataway, NJ). The mean sensitivities of these assays are 8.66 ng/ml for FSH and 0.1 ng/ml for LH.

Preparation and treatment of MEF (mouse embryonic fibroblast) cells. MEF cells were prepared as described previously (29). Briefly, male and female

$Nrf2^{-/-}$ or Wt mice were paired and pregnancy was monitored. Embryos were obtained at the 18th day after pairing under aseptic conditions. Embryo heads were used to confirm Nrf2 genotypes by PCR. Tissues from the embryo bodies were cultured in Dulbecco's modified Eagle's medium with 10% fetal bovine serum at 37°C and 5% CO_2. When MEF cells grew out of the embryo tissue, the cells were collected for experiments. MEF cells from three embryos of each genotype were used for experiments. For treatment, MEF cells were plated at 50% confluence in complete medium and grown overnight; the cells were then treated with vehicle (sesame oil) or VCD (30 μM) for different times as indicated.

Measurement of cellular redox potential. Cellular redox potential was examined following the distribution and oxidation of RedoxSensor Red CC-1 (Molecular Probes, Eugene, OR) in mitochondria and/or lysosome as described previously (8). Briefly, cells were incubated with 1 to 5 μM RedoxSensor Red CC-1 and 1 μM Mito Tracker Green FM (Molecular Probes) for 10 min. The cells were then washed with phosphate-buffered saline (PBS) and examined under a Zeiss 510 laser scanning confocal fluorescence microscope (Carl Zeiss Inc., Thornwood, NY). Images were collected at a magnification of ×40 (0.64-μm pixel size) with excitation wavelengths of 488 and 543 nm to excite Mito Tracker Green FM (green) and RedoxSensor Red CC-1 (red) simultaneously. Differential staining of lysosomes by RedoxSensor Red CC-1 (red) and mitochondria by Mito Tracker Green FM and RedoxSensor Red CC-1 (yellow, double staining) was used to evaluate the redox potential of the cells. Image analysis of relative fluorescence intensity was performed with Optimus version 6.51 software (Media Cybernetics, Silver Spring, MD) as previously described (46).

TUNEL assay. Apoptosis in ovarian cells was determined by TUNEL assay with a TUNEL assay kit (Promega, Madison, WI) as previously described (42). The fragmented DNA of apoptotic cells was measured by catalytically incorporated fluorescein-12-dUTP at the 3′-OH end of the DNA with the enzyme terminal deoxynucleotidyltransferase (TdT) to form a polymeric tail in a TdT-mediated dUTP nick end-labeling process as previously described (13). Briefly, the formalin-fixed, paraffin-embedded ovary sections were deparaffinized in xylene, followed by rehydration through an ethanol gradient to distilled water. The slides were then incubated with protease type 1 (Sigma) diluted with PBS at a concentration of 4%. A positive control slide was prepared by incubation with DNase 1 (Sigma Aldrich Co., St. Louis, MO) for 30 min at room temperature. All slides were then incubated with the equilibration buffer for 10 min, during which time the reaction mixture per slide was prepared by addition of 10 μl of the nucleotide mixture to 90 μl of equilibration buffer and 2 μl of TdT enzyme, according to the manufacturer's instruction. The negative control slide received 2 μl of distilled water in place of 2 μl of TdT2 in the fluorescein-12-dUTP reaction mixture. The slides were then incubated for 1 h at 37°C in the dark. Propidium iodide (100 μl/slide; Sigma Aldrich Co., St. Louis, MO) was applied for 2 min as a counterstain to label nuclei red, after which slides were rinsed in distilled water and coverslipped with Prolong Antifade (Molecular Probes). Slides were kept at 4°C in the dark until examined. The slides were imaged with a Zeiss LSM 510 laser scanning confocal microscope (Carl Zeiss, Inc., Thornwood, NY) at a magnification of ×20. Propidium iodide labeling was detected with a 543-nm laser with an LP 560 filter (shown in red), and the positive apoptotic cells were detected with a 480-nm laser and a BP 500–530 filter simultaneously. Depending on the intensity of the propidium iodide staining, which may vary from slide to slide, the apoptotic cells will appear either green or yellow-green.

Multiparameter flow cytometry of apoptosis. Detection of apoptotic cells by multiparameter flow cytometry was performed as described by Telford et al. (41). The assay measures three characteristic changes of apoptosis: caspase activation, plasma membrane phosphatidylserine (PS) "flipping," and increase in cell membrane permeability. PhiPhiLux-G1D2 (PhiPhiG1D2; OncoImmunin, Inc., Gaithersburg, MD) is a fluorogenic substrate of caspases 3 and 7. 7-Aminoactinomycin D (7-AAD; BD Bioscience, San Diego, CA) is used as an indicator of plasma membrane permeability. Annexin V-PE (BD Bioscience) binds to flipped PS in the plasma membrane. Briefly, cells were grown to 90% confluence and treated with VCD at a concentration of 0.5, 1, or 2 mM for 18 h. Cadmium (at 5 or 10 μM) was used as a positive control for apoptosis. All cultured cells were then collected and resuspended in medium at a density of $\sim 3 \times 10^6$/ml. A 50-μl volume of the cell suspension was mixed with 50 μl of 10 μM PhiPiD1G2, followed by incubation at 37°C for 60 min. A 1.25-μl sample of annexin V-PE was added to the mixture, which was incubated at room temperature for 15 min. The cells were washed with 1 ml of fluorescence-activated cell sorter (FACS) buffer (0.2% bovine serum albumin and 0.09% NaN_3 in PBS), collected by centrifugation, and resuspended in 250 μl of FACS buffer. The cells were incubated with 7-AAD (0.06 mg/1.25 ml/tube) at room temperature for 10 min. A 200-μl volume of FACS buffer was added to the tube immediately before measurement with a FACScalibur flow cytometer (Becton Dickinson, San Diego, CA).

Immunofluorescent staining and microscopy. Ovaries were fixed for 8 to 12 h in 4% buffered-formalin, dehydrated, and embedded in paraffin. Five-micrometer sections were deparaffinized through xylene and alcohol, rehydrated, and washed three times in a buffer consisting of PBS, 10% goat or rabbit serum, and 0.1% Tween 20. Sections were incubated with primary antibodies against Foxo3a at a 1:50 dilution in a humidified chamber overnight. Sections were washed in a buffer solution and incubated in the dark for 2 h with Cy5-conjugated secondary antibodies against rabbit immunoglobulin G at a 1:100 dilution (Chemicon International, Temecula, CA). Sections were then washed with PBS, followed by nuclear staining with YOYO-1 (Molecular Probes) at a 1:100 dilution for 20 min. After extensive washing with PBS, tissue sections were mounted on slides with Prolong Antifade. Stained sections were stored at 4°C in the dark and examined for fluorescence intensity within 1 week. Stained sections were examined on a Zeiss 510 laser scanning confocal microscope. Images were taken at magnifications of both ×20 (1.27-μm pixel size) and ×40 (0.64-μm pixel size) with excitation wavelengths of 488 and 633 nm to excite YOYO-1 nuclear staining (green) and Cy5 (red) simultaneously. Image analysis to quantify relative fluorescence intensity was performed with the Optimus version 6.51 software. Three sections were analyzed in each experimental group. No autofluorescence was seen in unstained ovarian sections at the 633-nm wavelength.

Induction of Nrf2 target genes. Wt and $Nrf2^{-/-}$ mice (2 months old) were treated with 3-*t*-butyl-4-hydroxyanisol (BHA), benzo[*a*]pyrene (Bap), or vehicle. BHA was given by intragastric administration on the first and third days at 400 mg/kg of body weight; Bap was given once by i.p. injection. Liver samples were collected on the fourth day after BHA treatment or 24 h after Bap treatment. For gene induction in cultured cells, hepa1c1c7 cells were grown to confluence and treated with VCD as described above for MEF cells. Total RNAs or total cell extracts were prepared for analyses of mRNA expression and protein levels, respectively.

RNA preparation and Northern blotting. Fresh tissues were stored in RNA Later (QIAGEN, Valencia, CA) at −20°C. Tissues were homogenized with zirconia beads (Biospec Products, Bartlesville, OK) in a bead beater (Med Associates, Inc., Georgia, VT). Total RNA was prepared with the RNeasy kit (QIAGEN). Total RNA (5 μg/lane) was fractionated in a 1% agarose-formaldehyde gel and transferred to a Nytran membrane. The blot was probed with a digoxigenin-labeled riboprobe specific for mouse NQO1, mEH, HO-1, MT-1, Foxo3a, or actin and visualized by chemiluminescence with a DIG RNA detection kit with CDP Star as the substrate (Roche Molecular Biochemicals).

Immunoblotting. Total cell lysates were prepared with cell lysis buffer (Promega, Madison, WI). Levels of Foxo3a protein were measured by immunoblotting with anti-FKHRL1 (Upstate) by following procedures provided by the manufacturer. Levels of Nrf2 protein were assayed with anti-Nrf2 antibodies from Santa Cruz Biotechnology, Inc. (Santa Cruz, CA).

Statistical analyses. Statistical analyses were performed with GraphPad Prism software (GraphPad Software, San Diego, CA). Data represent means and standard deviations. One-way analysis of variance (ANOVA) and Tukey's multiple comparison were performed for testing statistical significance at $P < 0.05$.

RESULTS

Depletion of ovarian primary and primordial follicles by VCD in $Nrf2^{-/-}$ mice. Wt and $Nrf2^{-/-}$ female mice at PND 28 were continuously treated with VCD at 0.57 mmol/kg of body weight per day for 15 days. VCD at this dose reduced the primordial follicle number by 50% and the primary follicle number by 60% of control numbers in Wt mice (Fig. 1A and B). A small but insignificant increase in secondary follicle numbers in the VCD-treated group was observed. Morphologically, the surviving follicles (small and large) were similar in structure between oil- and VCD-treated mice (Fig. 1A). The data suggest that VCD selectively destroys small follicles (primordial and primary) compared with large follicles (preantral and antral). Treatment of $Nrf2^{-/-}$ mice with VCD under the same regimen depletes the primordial and primary follicles by 96 and 95% of the control levels, respectively. Preantral or antral follicles are reduced by 30% in VCD-treated $Nrf2^{-/-}$ mice compared with oil control mice. Thus, loss of Nrf2 dramatically

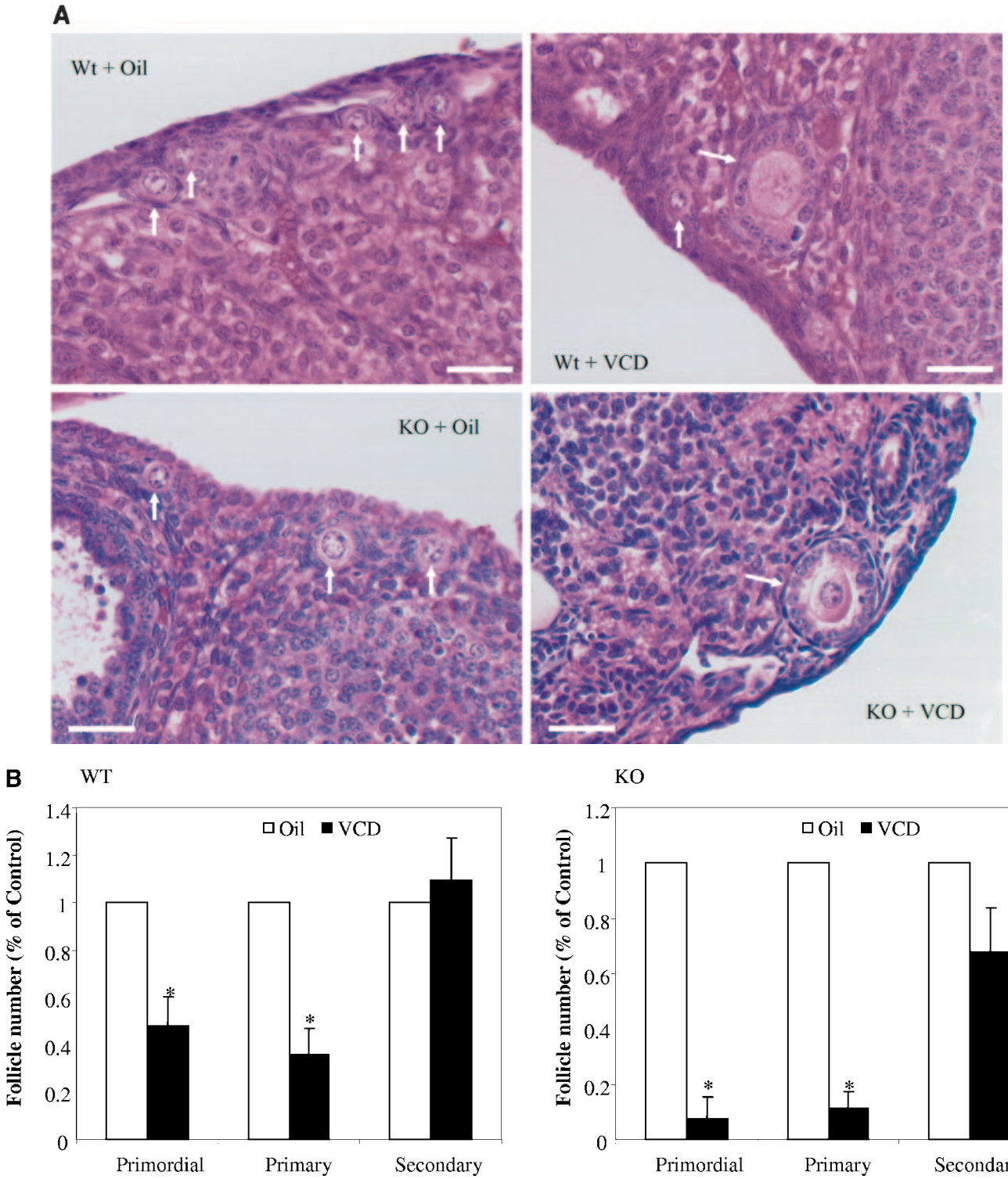

FIG. 1. Depletion of small follicles in Wt and Nrf2$^{-/-}$ mice by VCD. Female Wt and Nrf2$^{-/-}$ (KO) mice (28 days old) were treated with VCD or oil for 15 days as described in Materials and Methods. Ovarian sections were stained with H&E. Follicle morphology and numbers were examined under a microscope. (A) H&E-stained sections showing the morphology of follicles among different groups with largely reduced numbers of small follicles in VCD-treated Wt and Nrf2$^{-/-}$ mice. Arrows indicate primordial and primary follicles. (B) Quantification of follicle numbers. Statistical analysis was performed with the original data expressed as numbers of follicles per ovary ($n = 6$). *, $P < 0.05$. The data shown are percentages of controls for clarity of comparison. Bars = 30 μm.

increased the sensitivity of ovarian follicles to VCD ovotoxicity.

Mammalian follicle growth is irreversible. Most activated follicles will not reach the stage of ovulation but undergo apoptotic death (i.e., atresia), whereas unactivated follicles remain dormant. The observation that VCD destroys small follicles without causing apparent structural changes in the remaining follicles implicates apoptosis as a mechanism of follicle depletion analogous to atresia. To test this concept, we first examined if VCD caused apoptosis in cultured cells. hepa1c1c7 cells, of a murine hepatoma cell line that retains most of the characteristics of hepatocytes and is highly responsive to Nrf2 activators, were treated with VCD for 18 h. Apoptotic cells were detected by multiparameter flow cytometry. Figure 2 shows the fractions of cells undergoing apoptosis that are stained with PhiPhiG1D1 (indicator of caspase 3 or 7 activation), 7-AAD (reflecting increased membrane permeability), or annexin V (indicating plasma membrane PS flipping). As a positive control, cadmium at 5 or 10 μM was shown to increase cell fractions positive for staining with 7-AAD and PhiPhiG1D2 or annexin V and PhiPhiG1D2. Treatment with VCD at 0.5, 1, or 2 mM resulted in a dose-dependent increase in apoptosis compared with the control. VCH, which is the metabolic precursor of VCD, did not cause cell death or apoptosis of the cells at 2 mM under the same conditions. The results demonstrate, for the first time, that VCD, but not VCH, induces apoptosis in cultured cells; this finding is in agreement with the observation that VCD has an order of magnitude greater in vivo ovarian toxicity than VCH.

We then examined if VCD induces apoptosis of follicular cells in vivo. Figure 3 shows that apoptotic cells were seen mostly in large growing follicles compared with small follicles in untreated ovaries (Wt + oil, KO + oil). Treatment with VCD increased apoptotic cell numbers in follicles of Wt mice (Wt + VCD), and more apoptotic cells were seen in Nrf2$^{-/-}$ ovaries with VCD treatment (KO + VCD). The observation that more apoptotic cells were seen in large than small follicles in VCD-treated mice is attributable to the finding that a majority of the small follicles susceptible to VCD toxicity have been depleted by VCD. Alternatively, this result implies that VCD depletes small follicles by accelerating the growth of small follicles to large follicles, leading to apoptosis in a process similar to atresia. This notion is supported by the observations that treatment with VCD consistently increased the numbers of large follicles while decreasing those of the primary and primordial follicles both in intact animals (Fig. 1B, left side) and in cultured ovaries in vitro (9).

POF caused by VCD in Nrf2 null mice. The finding that VCD depletes ovarian follicles raises the question of whether such depletion leads to POF in intact animals. We tested this possibility with a continuous-breeding assay. Female Wt and Nrf2$^{-/-}$ mice were treated with VCD or oil. The mice were then paired with healthy Wt male mice for breeding starting at 6 weeks of age. Litter size was recorded, and pairing was continued until no birth was observed for each female. Figure 4A reveals that Wt mice exhibited an age-dependent decline in average litter size, reaching infertility at an age of ~50 weeks. Nrf2$^{-/-}$ mice had smaller litter sizes than Wt mice at younger ages (<30 weeks old). Treatment with VCD dramatically reduced litter size in Nrf2$^{-/-}$ mice, giving rise to zero birth at ~30 weeks of age. In the Wt, the cumulative number of progeny mice per female was decreased by VCD by ~25% at an age of 50 weeks (Fig. 4B). Nrf2$^{-/-}$ mice produced fewer progeny mice than did Wt mice at all ages; the cumulative number of progeny mice produced by the Nrf2$^{-/-}$ mice is ~75% of the Wt by 50 weeks of age. VCD reduced the cumulative number in Nrf2$^{-/-}$ mice to ~35% of the control (Wt, Oil) at an age of 50 weeks. These findings demonstrate, for the first time, that VCD reduces reproductive capacity in mice and causes secondary infertility in Nrf2 null mice, possibly due to their high sensitivity to the ovotoxicity of VCD. The correlation between the severity of follicle depletion and induction of infertility supports the concept that global damage of follicles by ovarian toxicants can result in POF.

Under normal physiological conditions, premature reduction of ovarian function elicits hypergonadotropic responses. FSH and LH levels were examined at 20 weeks of age after treatment with VCD or oil. Compared with oil controls, VCD significantly increased LH levels in Wt mice (Fig. 5A; $P < 0.05$) and both FSH and LH levels in Nrf2$^{-/-}$ mice (Fig. 5A and B; $P < 0.001$). A small but insignificant reduction of FSH in VCD-treated Wt mice was observed. Together, the results indicate that pituitary responses to follicle destruction exist in VCD-treated mice; depletion of follicles by VCD induces hypergonadotropic hypogonadism secondary to POF in Nrf2 null mice.

Accelerated ovarian follicle development during early age stages of Nrf2 null mice. The observation that Nrf2$^{-/-}$ mice are highly sensitive to VCD ovotoxicity implies a role for Nrf2 in ovarian follicular development under physiological conditions. Ovaries were collected from Wt and Nrf2$^{-/-}$ mice at PND 3, 8, 15, and 53, representing different stages of ovarian development (14). As shown in Fig. 6A, both genotypes contained primary and primordial follicles at PND 3. A pool of fully formed small follicles was seen at PND 8, whereas antral follicles were formed at PND 15. At PND 53, all stages of follicular development were observed, indicating sexual maturity.

The morphologies of the follicles appeared similar in both Wt (left) and Nrf2$^{-/-}$ (right) ovaries. However, the numbers of primordial and primary follicles exhibited a biphasic variation, increasing from PND 3 to 8 and decreasing from PND 8 to 53 (Fig. 6B, upper part). Moreover, more small follicles were formed at PND 3 and 8 in Nrf2$^{-/-}$ than in Wt mice. This trend was reversed between PND 8 and 53, during which considerably fewer small follicles were seen in Nrf2$^{-/-}$ than in Wt mice, suggesting accelerated, age-dependent follicular development and loss of small follicles in Nrf2$^{-/-}$ ovaries. The numbers of large follicles (preantral or antral follicles) were significantly increased at PND 8 and 15 in Nrf2$^{-/-}$ mice compared with the Wt (Fig. 6B, lower part), further supporting the notion that loss of Nrf2 function accelerates follicular development in mice.

Reduced basal and inducible expression of mEH. VCD can be metabolized to less toxic metabolites by phase II enzymes in the liver; conversion of VCD to dio and tetrio metabolites by mEH is a key step in VCD detoxification (17). In view of the importance of Nrf2 in phase II gene regulation and the high sensitivity of Nrf2 null mice to VCD toxicity, we examined the expression and induction of mEH in Nrf2 null mice. As shown

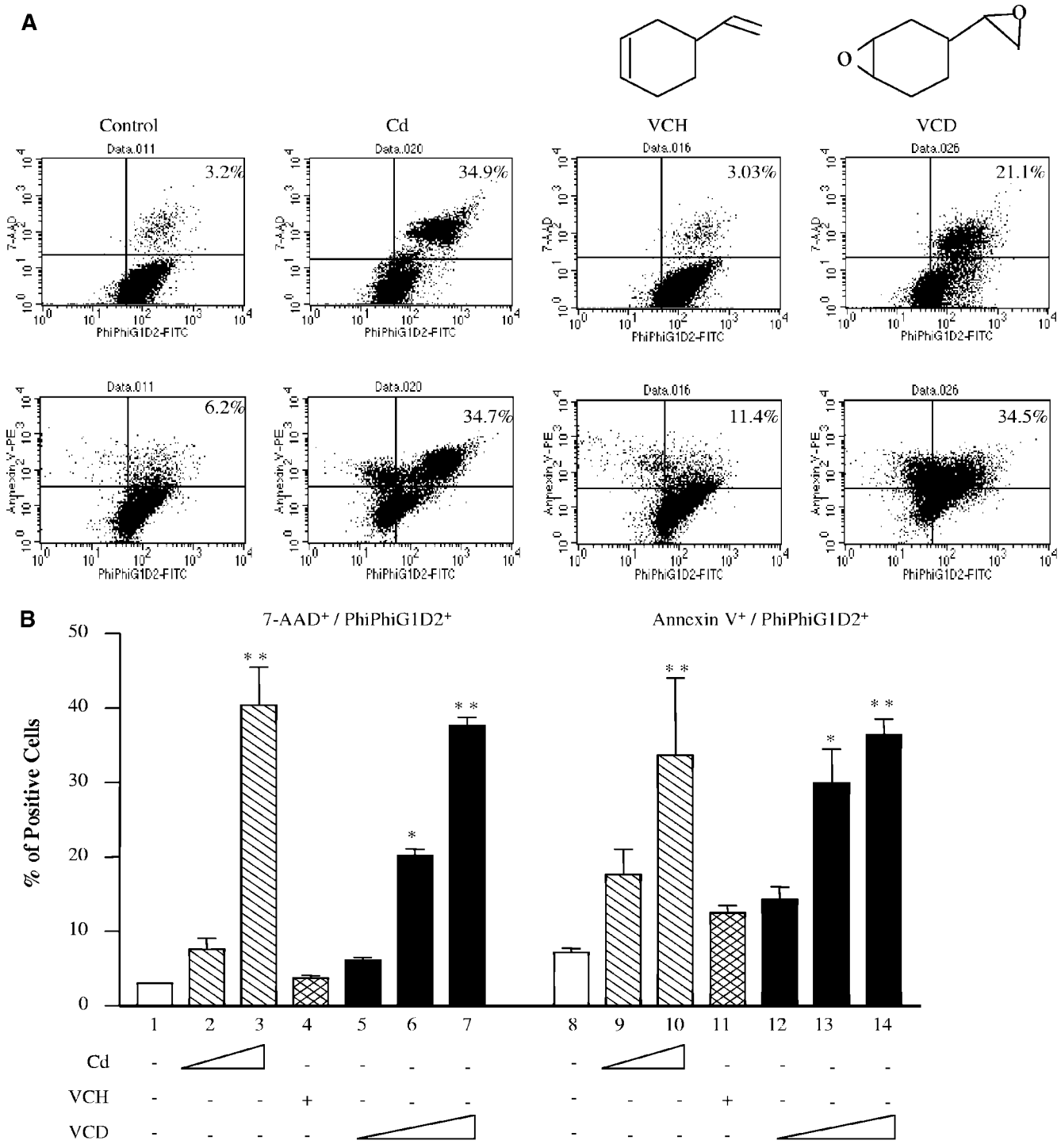

FIG. 2. Multiparameter flow cytometry of apoptosis by VCD. hepa1c1c7 cells at ~90% confluence were treated with Cd (positive control), VCD, or VCH for 16 h at 37°C. The cells were harvested and stained with PhiPhiG1D2, 7-AAD, or annexin V-PE as described in Materials and Methods. Apoptotic cells were detected by multiparameter flow cytometry as cells positive for staining with 7-AAD and PhiPhiG1D2 or annexin V and PhiPhiG1D2. (A) Distribution of apoptotic cells. Shown at the top are the structures of VCH and VCD. Cd, 10 μM; VCH, 2 mM; VCD, 1 mM. (B) Data from panel A shown as percentages of double-positive cells. Cells were treated with vehicle only (lanes 1 and 8), with Cd at 5 μM (2 and 9) or 10 μM (3 and 10), with VCH at 2 mM (4 and 11), or with VCD at 0.5 mM (5 and 12), 1 mM (6 and 13), or 2 mM (7 and 14). Means and standard deviations were calculated by one-way ANOVA, followed by a comparison of individual means. The symbols * and ** represent $P < 0.05$ and $P < 0.01$, respectively, in comparison with the control values.

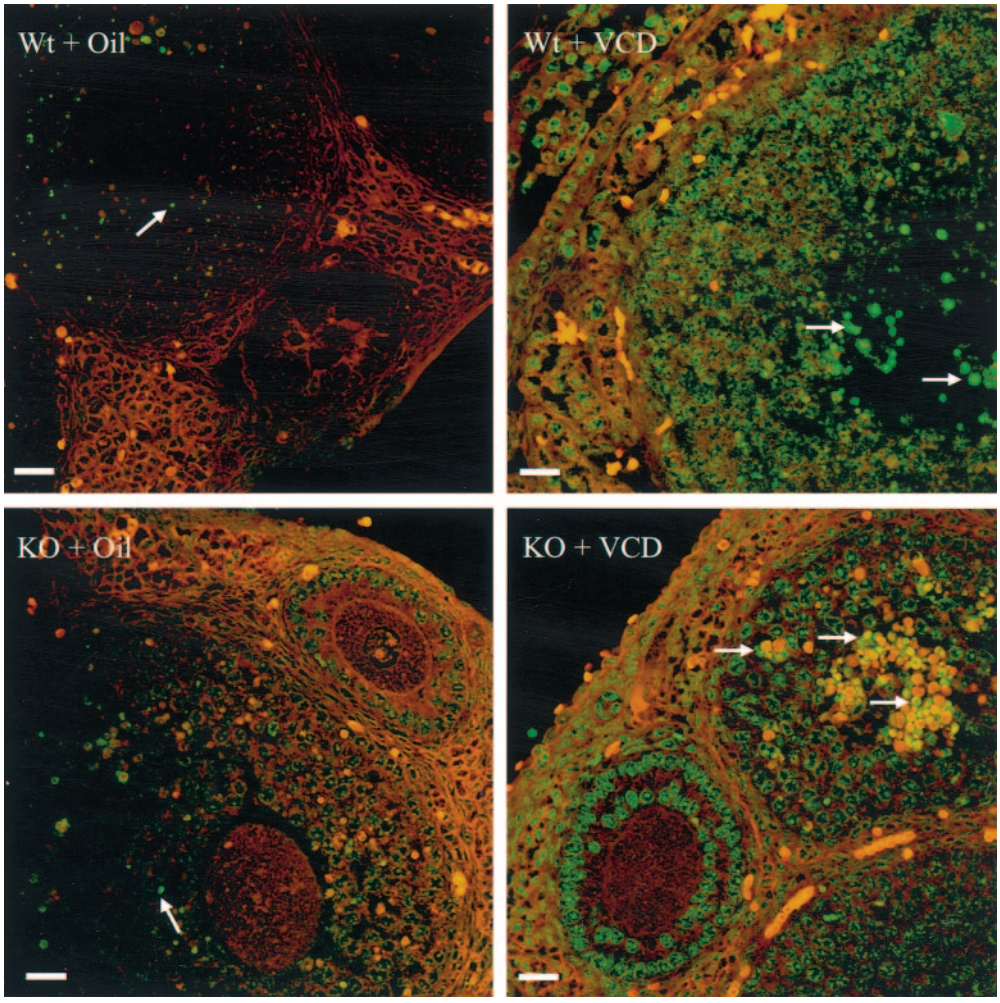

FIG. 3. Confocal micrographs of TUNEL assays of ovarian follicles. TUNEL assays were performed on ovarian tissue sections from Wt mice treated with oil (Wt + Oil) or VCD (Wt + VCD) and KO mice treated with oil (KO + Oil) or VCD (KO + VCD). Cells positive for apoptosis appear bright green-yellow (arrow), and the propidium iodide counterstain labels the cells red. Increased numbers of cells stained green or yellow in KO + VCD tissue suggest more severe apoptosis in Nrf2 KO ovaries. Bars = 50 μm.

in Fig. 7, mEH exhibited a high level of constitutive expression in the Wt liver (upper part, lanes 7 and 8) and was induced moderately by Bap (lanes 9 and 10) and BHA (lanes 11 and 12). However, the basal expression was largely reduced and the induction was abolished in the Nrf2$^{-/-}$ liver (lanes 1 to 6). As a control for Nrf2 function, NQO1 mRNA was shown to be highly induced by Bap and BHA (middle part, compare lanes 9 and 10 or 11 and 12 with lanes 7 and 8), but the induction was totally lost in Nrf2$^{-/-}$ mice (lanes 1 to 6). Actin mRNA was measured as a loading control (lower part). These findings implicate Nrf2 as a major regulator of the basal and inducible expression of mEH. Thus, loss of Nrf2 function decreases the hepatic expression of mEH and other phase II genes, leading to reduced detoxification and, consequently, increased toxicity of VCD in Nrf2$^{-/-}$ mice.

Increased oxidative response and activation of Nrf2 by VCD. Nrf2 is associated with ROS defense. Induction of oxidative stress by VCD was examined by measuring reduction-oxidation capacities of cells, induction of oxidative stress marker genes in the ovary, and activation of Nrf2. RedoxSensor Red CC-1 is a new redox-sensitive fluorescent probe that preferentially localizes between mitochondria and lysosomes, reflecting the cytoplasmic redox potential of a cell. In Wt embryonic fibroblasts, a high red to yellow fluorescence ratio (representing the ratio of lysosomal to mitochondrial staining) was observed, indicating a low oxidative state in the cell (Fig. 8A, upper left part, and B, Wt + Oil). The ratio was significantly reduced in Nrf2$^{-/-}$ cells (Fig. 8A, lower left part, and B, compare KO + Oil with Wt + Oil; $P < 0.001$), reflecting increased oxidative stress in Nrf2 null cells. Treatment with VCD reduced the ratio in the Wt, and the reduction was further enhanced in Nrf2 null cells (Fig. 8A, upper and lower right parts, and B, Wt + VCD and KO + VCD). The findings not only demonstrated increased oxidative stress by VCD but also suggested a synergy between VCD and Nrf2 null function in promoting ROS production.

Next, we examined if VCD induced the expression of oxidative stress marker genes such as those that encode HO-1 and MT-1. As shown in Fig. 9A, VCD dramatically increased the mRNA expression of oxidative markers HO-1 (upper part) and

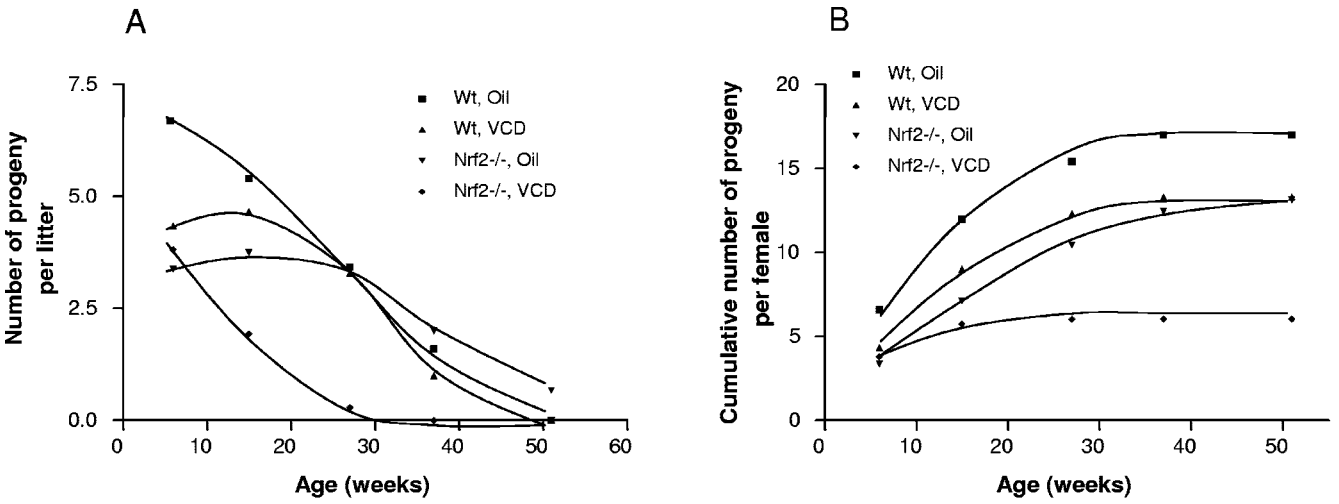

FIG. 4. Accelerated premature reproductive failure in VCD-treated Nrf2 null mice. Female Wt (C57BL/6, eight per group) and Nrf2$^{-/-}$ (six per group) mice 28 days old were treated with VCD or a vehicle control by i.p. injection once daily for 15 days as described in Materials and Methods. Continuous-breeding assays began at 6 weeks of age, in which VCD- or vehicle-treated females were paired with age-matched, healthy Wt male mice. Litter sizes were recorded, and females were re-paired with different males after offspring mice were weaned. When no birth was observed, the female was paired with a healthy male one more time to ensure that complete loss of reproductive function was reached. (A) Decline in the average number of progeny mice per litter. (B) Cumulative number of progeny mice per female.

MT-1 (middle part) in hepa1c1c7 cells. We then analyzed the regulation of HO-1 mRNA expression in the ovaries of intact animals. VCD induced HO-1 expression in Wt ovaries (Fig. 9B, compare lanes 1 and 2). However, the basal expression of HO-1 was largely reduced and induction by VCD was totally lost in Nrf2$^{-/-}$ ovaries. These findings suggest that VCD induces oxidative stress and subsequently induces HO-1 transcription in the ovaries through an Nrf2-dependent pathway.

Oxidative signals activate Nrf2 by stabilizing the protein. Induction of oxidative stress and HO-1 gene expression by VCD suggests activation of Nrf2 during VCD treatment. Figure 9C shows that the protein level of Nrf2 was largely reduced by treatment with protein synthesis inhibitor cycloheximide (CHX), indicating a highly labile nature of the Nrf2 protein (compare lane 2 with lane 1). VCD increased the level of Nrf2 protein (lane 3). *tert*-Butylhydroquinone (tBHQ), a redox-cycling antioxidant and a known activator of Nrf2, and MG132, an inhibitor of 26S proteasome-mediated Nrf2 degradation, stabilized the Nrf2 protein as expected (lanes 5 and 7). The results suggest that VCD stabilizes Nrf2 similarly to oxidative or antioxidant stimuli, which accounts for the induction of HO-1 in the ovaries by VCD. Taken together, the findings

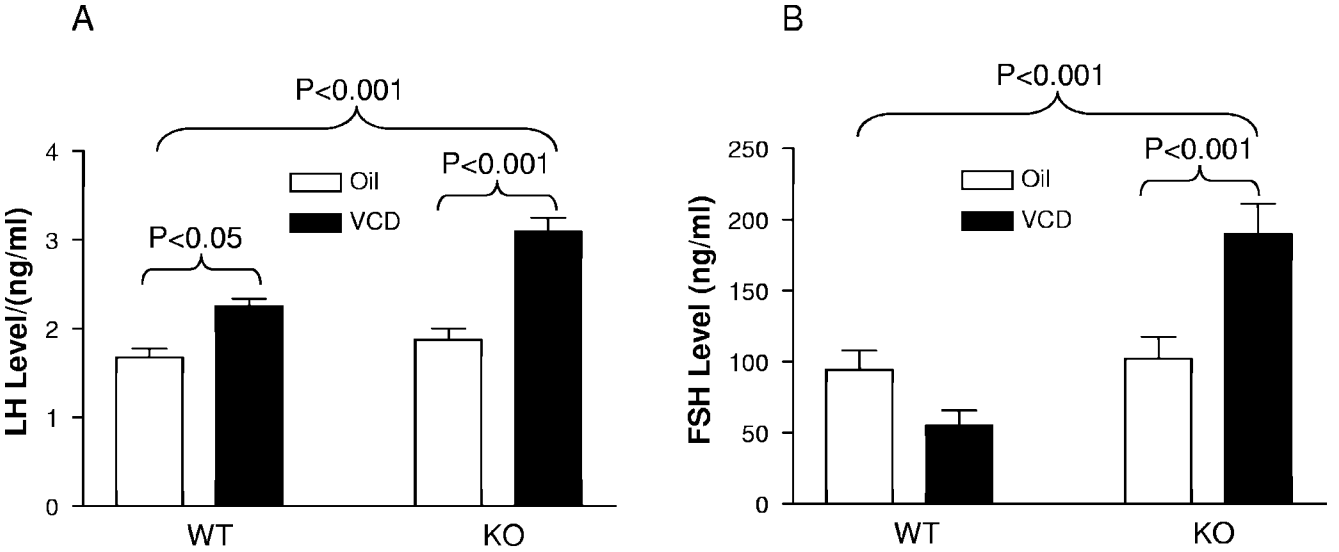

FIG. 5. Hormonal effects of VCD. Female Wt and Nrf2 KO mice (28 days old) were dosed daily with VCD or sesame oil for 15 days as described in Materials and Methods. Twenty weeks later, plasma LH (A) and FSH (B) levels were measured by a competitive enzyme immunoassay method. The mean sensitivity was 8.66 ng/ml for FSH and 0.44 ng/ml for LH. For all panels, data are represented as the mean ± the standard deviation; $n = 8$ (C57BL/6) or 6 (Nrf2$^{-/-}$).

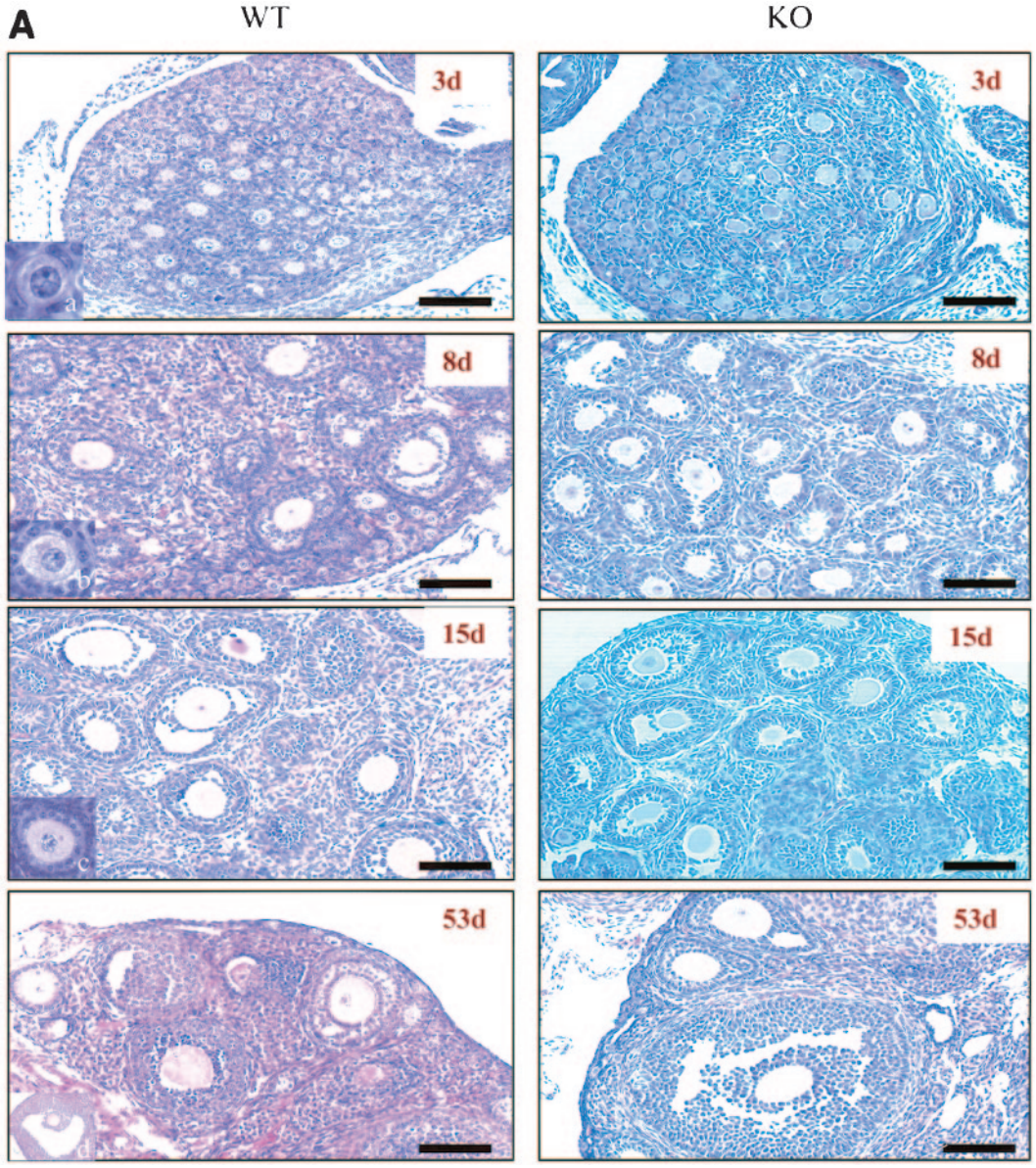

FIG. 6. Accelerated follicle development in early age stages of Nrf2$^{-/-}$ mice. Ovaries were collected from Wt and Nrf2$^{-/-}$ mice at different ages, serially sectioned (7 μm), and stained with H&E. (A) Micrographs generated with an oil immersion objective (bars = 50 μm) showing increased numbers of antral follicles in ovaries from Nrf2$^{-/-}$ mice at 8 and 15 days compared with the Wt. Inserts show typical primordial (a), primary (b), small growing (c), and preantral (d) follicles. (B) Quantitation of follicles. Follicles at different developmental stages were counted as described in Materials and Methods. Data represent means ± standard deviations of follicle numbers per ovary from six mice per group. One-way ANOVA and Turkey's comparison test were performed for statistical analysis. *, $P < 0.05$.

demonstrate that VCD induces oxidative stress, as well as Nrf2-dependent protective responses against ROS, in the ovaries. Therefore, induction of high levels of oxidative stress by VCD in ROS defense-compromised Nrf2$^{-/-}$ cells contributes to increased ovarian toxicity of VCD in Nrf2$^{-/-}$ mouse ovaries.

Interplay between Nrf2 and Foxo3a signaling in follicle development and VCD action. Foxo3a, a member of the forkhead transcription factor family, has been implicated in the suppression of early-stage follicular growth; deletion of the Foxo3a gene results in a distinctive ovarian phenotype characterized by global follicular activation, followed by early depletion of functional ovarian follicles and secondary infertility (5, 16). The observations of selective destruction of small follicles by VCD (Fig. 1) and increased follicular growth in Nrf2$^{-/-}$ mice during PND 3 to 15 (Fig. 6) prompted us to examine a role for VCD and Nrf2 in the regulation of Foxo3a expression.

In Wt follicles, Foxo3a was readily detected in both the cytoplasm and nuclei of follicular cells by immunofluorescent staining (Fig. 10A, upper left part, red). Foxo3a expression was significantly reduced in follicles from Nrf2$^{-/-}$ mice treated with oil (Fig. 10A, bottom left part) compared to the Wt (Fig. 10A, top left part). Quantification of fluorescent staining is shown in Fig. 10B. The result implies Nrf2-dependent regula-

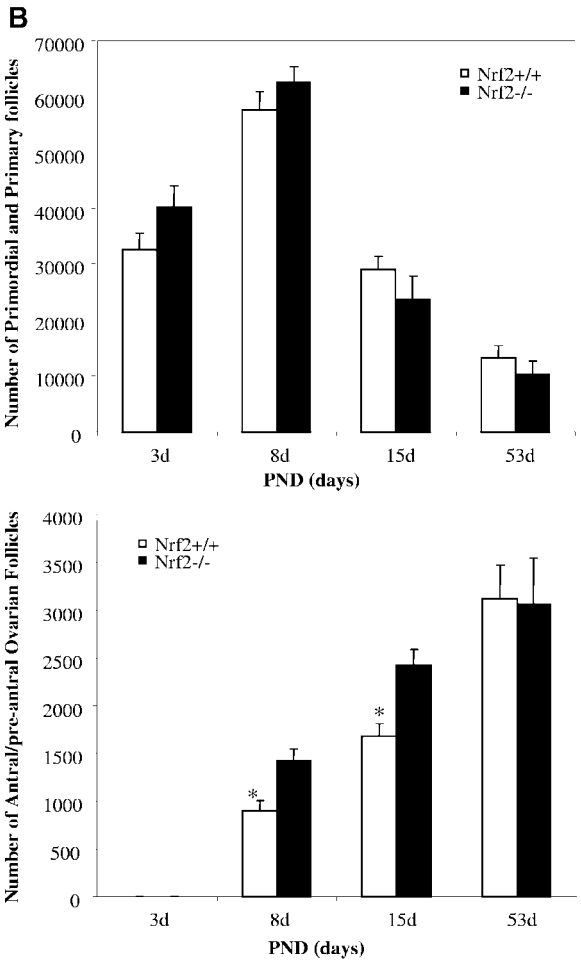

FIG. 6—*Continued.*

tion of Foxo3a expression in normal ovaries and suggests reduced Foxo3a expression as a cause of the accelerated follicular growth observed in Nrf2$^{-/-}$ mouse ovaries. Treatment with VCD significantly increased the expression of the Foxo3a protein in Wt follicles (Fig. 10A, upper right part, red, and B, Wt + VCD; $P < 0.001$). This increase was further elevated in Nrf2$^{-/-}$ mouse ovaries (Fig. 10A, lower right part, and B, KO + VCD; $P < 0.001$). Thus, VCD and Nrf2 null function exhibit synergy in elevating Foxo3a expression in follicle cells at the protein level.

To further analyze the mechanism of Foxo3a regulation, the expression of its mRNA was examined by Northern blotting. In Fig. 11A, VCD was shown to induce Foxo3a mRNA in hepa1c1c7 cells. Induction of Foxo3a mRNA was observed in VCD-treated Wt ovaries, which is in agreement with an elevated Foxo3a protein level in the ovaries (Fig. 10A, Wt + VCD). However, the basal expression and induction of Foxo3a mRNA were largely diminished in Nrf2$^{-/-}$ ovaries. The induction of Foxo3a by VCD in Wt ovaries and its decreased expression in KO ovaries were analogous to those of HO-1 and NQO1 in the liver and ovaries, indicating that Nrf2 regulates the basal expression and induction of Foxo3a mRNA in ovarian follicles. The discrepancy between the reduced Foxo3a mRNA expression and the increased level of Foxo3a protein caused by VCD in Nrf2$^{-/-}$ ovaries suggests an Nrf2-independent mechanism in the regulation of the Foxo3a protein by VCD. To address this question, regulation of Foxo3a in hepa1c1c7 cells was analyzed by immunoblotting. As predicted, VCD increased the level of Foxo3a protein (Fig. 11C, lane 2). Surprisingly, treatment with CHX largely reduced the basal expression of Foxo3a, indicating that Foxo3a is a labile protein. Treatment with MG132 increased the level of Foxo3a protein threefold. Together, these data provide the first evidence demonstrating that Foxo3a is regulated by degradation through the 26S proteasome pathway under physiological conditions. These findings suggest a mechanism of VCD-induced elevation of the Foxo3a protein in Nrf2$^{-/-}$ mouse ovaries by inhibition of the proteasomal degradation of the Foxo3a protein. Alternatively, loss of Nrf2 reduced the proteasomal degradation of Foxo3a in the ovaries. This notion is supported by a recent finding that Nrf2 serves as a positive transcriptional regulator of most subunits of the 20S and 19S proteasomes by directly binding to tandem AREs in the promoter regions of the subunits (25).

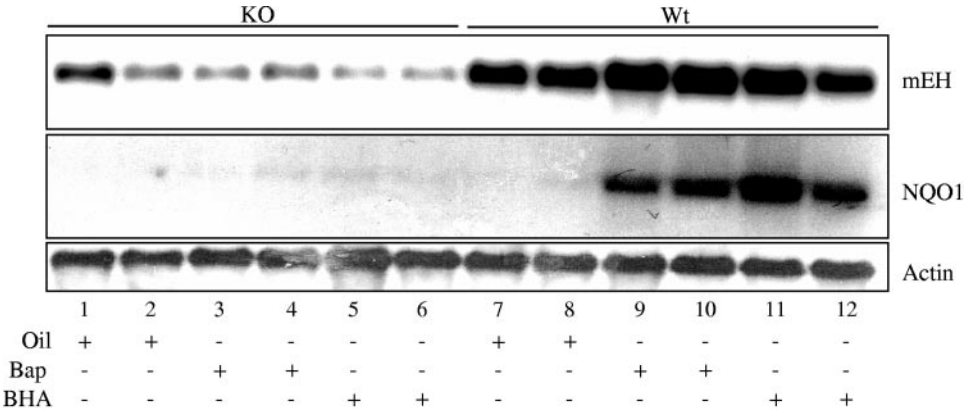

FIG. 7. Basal and inducible expression of mEH in Nrf2$^{-/-}$ mice. Wt (lanes 7 to 12) and Nrf2$^{-/-}$ (lanes 1 to 6) mice were treated with BHA (intragastrically), Bap (i.p.), or vehicle. Total RNA was prepared and analyzed for mEH and NQO1 basal expression and induction by Northern blotting. A parallel blot of the same samples was probed with an actin probe to ensure equal loading.

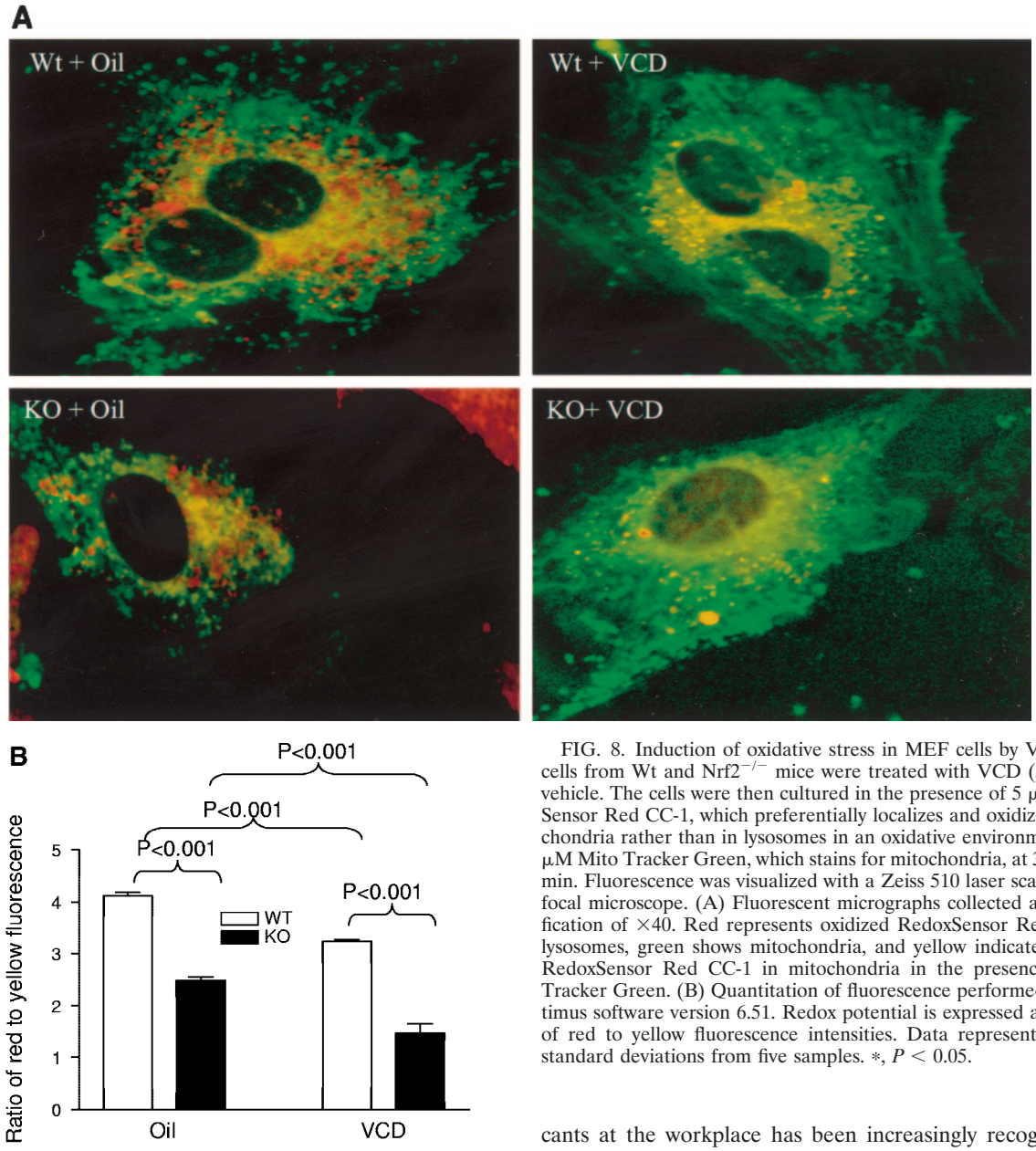

FIG. 8. Induction of oxidative stress in MEF cells by VCD. MEF cells from Wt and Nrf2$^{-/-}$ mice were treated with VCD (30 μM) or vehicle. The cells were then cultured in the presence of 5 μM RedoxSensor Red CC-1, which preferentially localizes and oxidizes in mitochondria rather than in lysosomes in an oxidative environment, and 1 μM Mito Tracker Green, which stains for mitochondria, at 37°C for 10 min. Fluorescence was visualized with a Zeiss 510 laser scanning confocal microscope. (A) Fluorescent micrographs collected at a magnification of ×40. Red represents oxidized RedoxSensor Red CC-1 in lysosomes, green shows mitochondria, and yellow indicates oxidized RedoxSensor Red CC-1 in mitochondria in the presence of Mito Tracker Green. (B) Quantitation of fluorescence performed with Optimus software version 6.51. Redox potential is expressed as the ratio of red to yellow fluorescence intensities. Data represent means ± standard deviations from five samples. *, $P < 0.05$.

DISCUSSIONS

POF, which is characterized by secondary infertility with persistently elevated gonadotropin levels before the age of 40, is a common cause of infertility and premature aging in women (1). The incidence of POF is estimated to be 1%. Although some POF cases have been associated with certain genetic factors, the etiology of the majority of POF cases remains unknown (1, 11, 32).

Exposure to certain environmental factors can lead to destruction of ovarian follicles in experimental animals and has been associated with POF in humans, including chemo- and radiotherapy in cancer patients, cigarette smoking, and occupational exposure to ovotoxicants such as 2-bromopropane (18, 33). The importance of protecting women from ovotoxicants at the workplace has been increasingly recognized for several reasons. More women have joined the workforce than ever before, and many working women postpone childbearing. POF would preclude this population from pregnancy at a late age. Lastly, new chemicals, materials, processes, and equipment are developed and marketed at an accelerating pace, presenting potentially new health hazards at work. Assessing chemical ovotoxicity remains a challenging task due to the lack of sensitive animal models and a poor understanding of the mechanism governing follicle activation and growth. In this study, we demonstrated that destruction of small follicles by the occupational chemical VCD reduces reproductive fitness. Ablation of Nrf2 dramatically increased VCD ovotoxicity, leading to early depletion of functional ovarian follicles and secondary infertility accompanied by hypergonadotropic hypogonadism. To our knowledge, this is the first report of an animal model of chemical-induced POF which may be useful in evaluating potential occupational and environmental chemi-

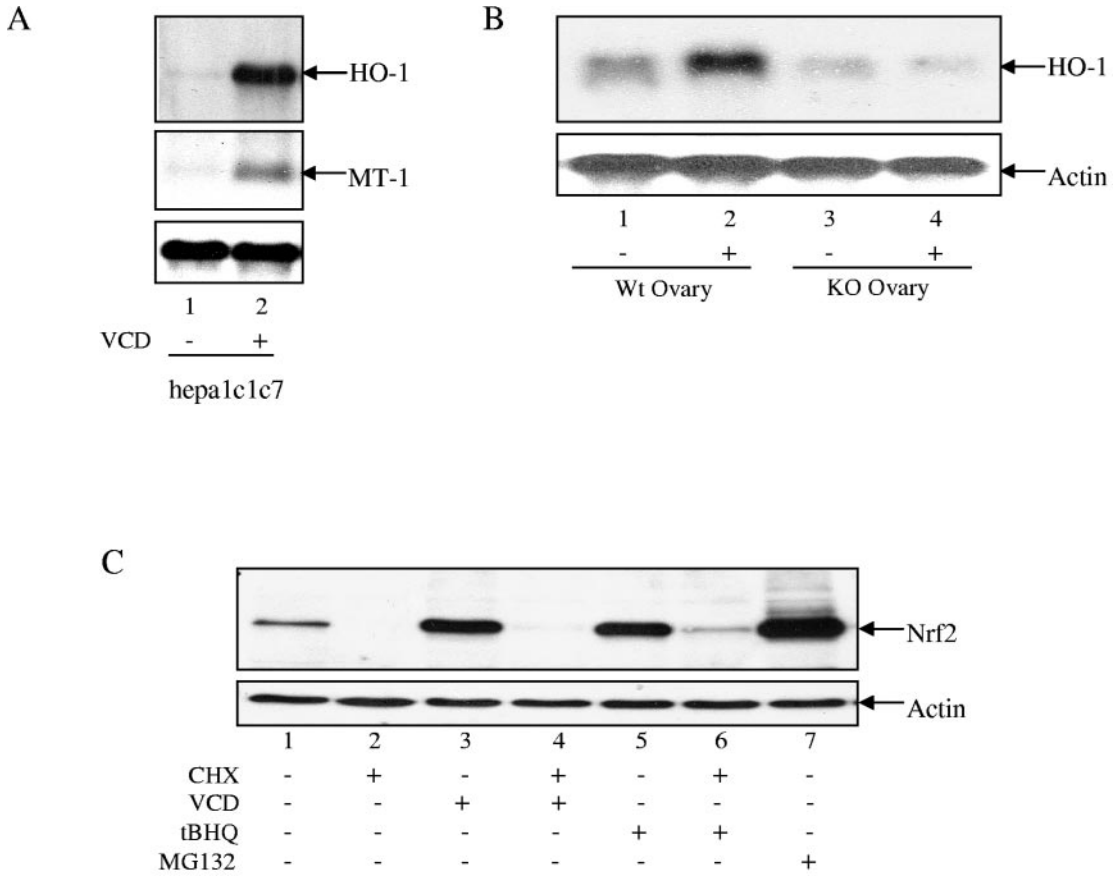

FIG. 9. Induction of oxidative marker genes and activation of Nrf2 by VCD. (A) Induction of HO-1 and MT-1 mRNA in hepa1c1c7. Cells were treated with VCD (30 μM) for 5 h. Induction was analyzed by Northern blotting. (B) Induction of HO-1 in the ovary. Female C57BL/6 and Nrf2$^{-/-}$ mice at an age of 28 days were treated with VCD at 0.57 mmol/kg of body weight per day by i.p. injection for 15 days. Ovaries from six mice of each treatment group were pooled for RNA preparation. Five micrograms of the total RNA of each mouse was analyzed for HO-1 expression by Northern blotting. (C) Immunoblotting. hepa1c1c7 cells were treated with VCD (30 μM), CHX (10 μg/ml), tBHQ (100 μM), or MG132 (25 μM) for 5 h. Five micrograms of the total cell lysate of each mouse was analyzed by immunoblotting with anti-Nrf2 antibodies.

cals that may be toxic to ovarian follicles in humans upon exposure.

Phase II enzymes consist of several classes of enzymes that catalyze the reduction and conjugation reactions of many xenobiotics, as well as endogenous chemicals, resulting in increased excretion and detoxification of the chemicals in most cases. Many phase II enzymes are constitutively expressed and can be induced by inducers in hepatic tissues and intestinal epithelial cells. We have used murine NQO1 as a model for a mechanistic study of transcriptional regulation of phase II genes. We have previously shown that Nrf2 is required for the basal expression and induction of mouse NQO1 by 2,3,7,8-tetrachlorodibenzo-*p*-dioxin (an aryl hydrocarbon receptor agonist) and tBHQ (a phenolic antioxidant). The results suggest that Nrf2 is a labile protein and serves as a master regulator which integrates physiological and environmental signals to regulate NQO1 expression (29). mEH catalyzes the hydration reactions of many epoxides, giving rise to dio metabolites. Metabolism of VCD by mEH to the inactive tetrio, i.e., 4-(1,2-dihydroxy)ethyl-1,2-dihydoxycyclohexine, is the first and critical step in VCD detoxification (17). Unlike NQO1, which is highly inducible, mEH exhibits a high level of constitutive expression in the liver and is moderately inducible by aryl hydrocarbon receptor agonists and phenolic antioxidants (Fig. 7) (27). The mechanism by which mEH is regulated at transcription levels is unclear. We have shown that loss of Nrf2 blocked mEH expression in the mouse liver in the absence and presence of mEH inducers, implicating Nrf2 as a key regulator of both basal and inducible expression of mEH in the liver. Others reported similar conclusions (37). By analogy with the findings of NQO1, it is postulated that Nrf2 recognizes ARE or ARE-like enhancers of mEH, thereby controlling mEH transcription.

Several lines of evidence implicate oxidative stress as a mechanism of VCD action and the high sensitivity of Nrf2$^{-/-}$ mice to VCD ovotoxicity. First, VCD was shown to increase the oxidative potential of MEF cells as directly measured by RedoxSensor Red CC-1 (Fig. 8). Second, VCD induced the expression of oxidative marker mRNAs such as HO-1 and MT-1 in hepatoma cells and in ovarian follicles of intact animals (Fig. 9A and B). Third, VCD activated Nrf2 and induced HO-1 and Foxo3a in the ovaries through an Nrf2-dependent pathway similarly to the induction of the genes by oxidative and antioxidant stimuli (Fig. 9B and 11B). Finally, loss of Nrf2

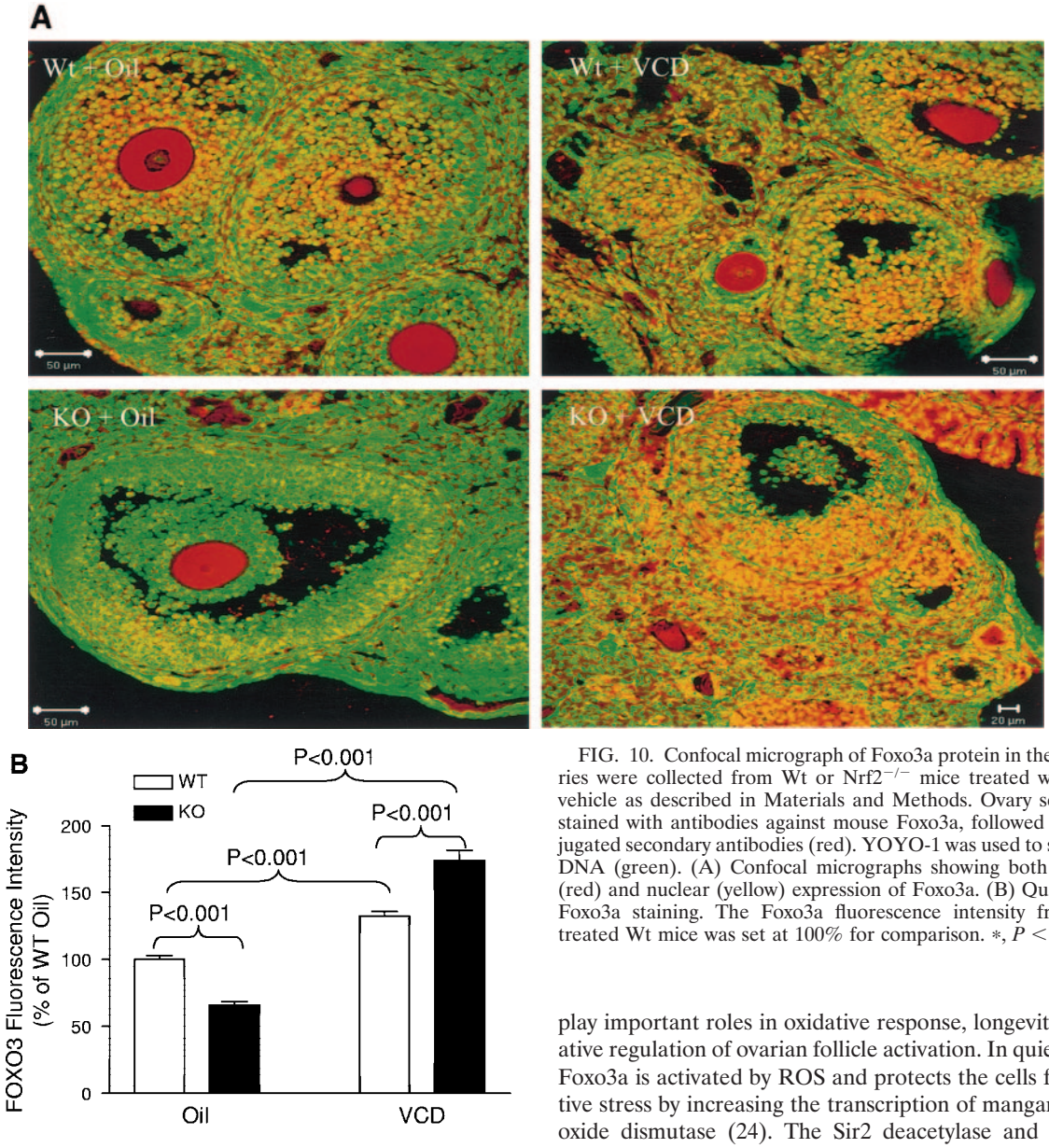

FIG. 10. Confocal micrograph of Foxo3a protein in the ovary. Ovaries were collected from Wt or Nrf2$^{-/-}$ mice treated with VCD or vehicle as described in Materials and Methods. Ovary sections were stained with antibodies against mouse Foxo3a, followed by Cy5-conjugated secondary antibodies (red). YOYO-1 was used to stain nuclear DNA (green). (A) Confocal micrographs showing both cytoplasmic (red) and nuclear (yellow) expression of Foxo3a. (B) Quantitation of Foxo3a staining. The Foxo3a fluorescence intensity from vehicle-treated Wt mice was set at 100% for comparison. *, $P < 0.05$; $n = 5$.

function further increased the oxidative potential induced by VCD, suggesting a synergistic action between VCD and an Nrf2 null function in promoting oxidative stress. This finding is in agreement with the notion that, in addition to regulating phase II genes, Nrf2 controls the expression of a battery of oxidative-stress-inducible genes critical in ROS defense, including those that encode HO-1 and MT-1 (Fig. 9), as well as *gcsH*, *gcsL*, and *gss* (6, 26). Taken together, these findings demonstrate that oxidative damage by VCD is a component of VCD toxicity and protection against VCD ovotoxicity by Nrf2 is at least in part attributable to the role of Nrf2 in ROS defense.

The Foxo subfamily of forkhead transcription factors includes Foxo3a (FKHRL1), Foxo1 (FKHR), Foxo4 (AFX), and the yeast protein DAF-16. Foxo proteins have been implicated in diverse biological functions (16). Foxo3a has been shown to play important roles in oxidative response, longevity, and negative regulation of ovarian follicle activation. In quiescent cells, Foxo3a is activated by ROS and protects the cells from oxidative stress by increasing the transcription of manganese superoxide dismutase (24). The Sir2 deacetylase and the *p66shc* locus modulate the organismal life span in different species. Sir2 acetylates Foxo3a and regulates Foxo3a functions in two ways: increasing the ability of Foxo3a to induce cell cycle arrest and resistance to oxidative stress and inhibiting its ability to induce cell death (4). The p66shc protein appears to regulate Foxo3a by controlling intracellular oxidant levels in cells, thereby affecting life span (35). Thus, Foxo3a is regulated by ROS and is critically involved in defense against oxidative stress during physiological processes such as aging. The critical role of Foxo3a in female reproductive function was unveiled in the study of targeted Foxo3a KO mice. Female mice with a Foxo3a$^{-/-}$ genotype exhibited global ovarian follicular activation leading to early depletion of ovarian follicles and POF, implicating Foxo3a as a critical repressor of ovarian follicle activation in the early stage of follicle growth (5, 16).

We found that Foxo3a expression is down-regulated in follicular cells in Nrf2$^{-/-}$ mouse ovaries, which correlates with accelerated growth of the follicles in the absence of exogenous

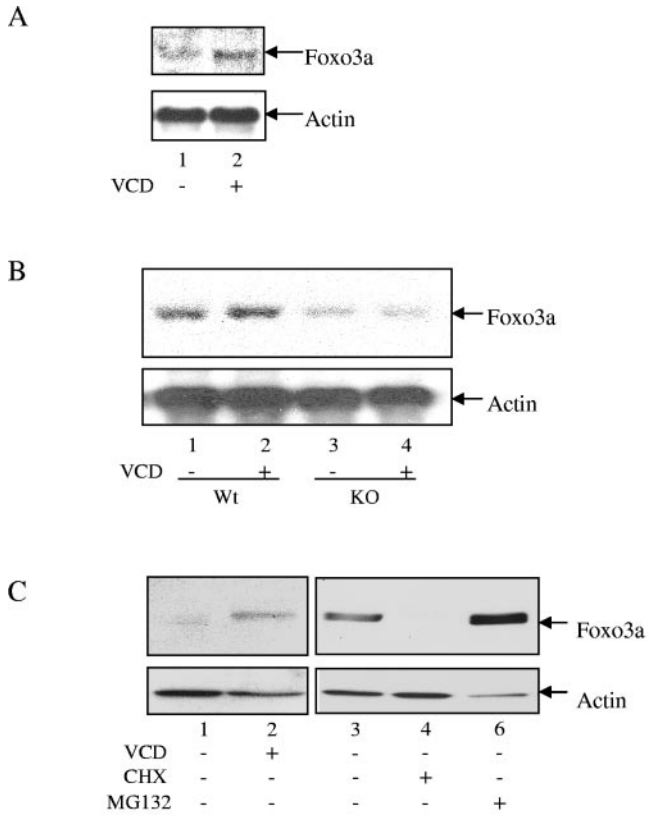

FIG. 11. Regulation of Foxo3a expression by VCD. (A) Induction of Foxo3a mRNA in hepa1c1c7 cells. Cells were treated with VCD as described for Fig. 9. Five micrograms of the total RNA of each mouse was analyzed for Foxo3a mRNA expression by Northern blotting. (B) Nrf2 dependence of Foxo3a mRNA expression in ovaries. Female Wt and KO mice were treated with VCD, and total RNA was prepared from ovaries pooled from six mice from each group as described for Fig. 9. Five micrograms of the total RNA of each mouse was analyzed for Foxo3a mRNA expression by Northern blotting. (C) Stabilization of Foxo3a protein. hepa1c1c7 cells were treated with VCD, CHX, or MG132 as described for Fig. 9. Total cell lysates were analyzed for Foxo3a protein by immunoblotting with polyclonal antibodies against mouse Foxo3a.

stimuli in Nrf2$^{-/-}$ mice. The observations imply that Nrf2 plays a role in the physiological regulation of follicular activation and growth by regulating the expression of Foxo3a in ovarian cells. On the other hand, treatment with VCD increases Foxo3a expression at both the mRNA and protein levels in follicular cells. Our data revealed that Foxo3a can be regulated through two pathways. In the first scenario, Foxo3a serves as a downstream target gene of Nrf2 involved in the maintenance of ovarian physiological functions and ROS defense. VCD induced Foxo3a mRNA transcription by stabilizing Nrf2 similarly to the induction of HO-1 by tBHQ. In this regard, an ARE or ARE-like enhancer element(s) could be involved in the induction. Detailed analyses of the upstream region of the gene are needed to identify the element(s) involved in the transcriptional regulation of Foxo3a by Nrf2. Secondly, we found that Foxo3a was degraded through the 26S proteasome pathway in the absence of exogenous chemicals. VCD increased the level of Foxo3a protein in Nrf2$^{-/-}$ mouse follicles even though the mRNA of Foxo3a was reduced in the ovaries. VCD stabilized Foxo3a in cultured cells similarly to tBHQ and MG132. Thus, our findings suggest a novel mechanism of Foxo3a regulation in which oxidative stress induced by VCD inhibits the proteasomal degradation of Foxo3a, thereby stabilizing the protein. In either of the cases, induction of Foxo3a as a result of VCD exposure represents an adaptive response to increased oxidative stress caused by VCD in ovary cells to protect the cells from damage by ROS. Given the critical roles of Foxo3a in follicle activation and ROS defense, our study provides new opportunities to understanding the interplay between the Nrf2 and Foxo3a signaling pathways and how it regulates the defense against xenochemicals, the biology of ROS, and follicular development in the ovary.

ACKNOWLEDGMENTS

We thank P. Nicolaysen for valuable suggestions on mouse breeding assay, S. Young for assistance in FACS analysis, J. Antonini and J. Yao for NIOSH internal review, I. D. Clair for comments, and P. A. Willard for histopathological sample preparation.

The findings and conclusions in this report are ours and do not necessarily represent the views of NIOSH.

REFERENCES

1. **Anasti, J. N.** 1998. Premature ovarian failure: an update. Fertil. Steril. **70:**1–15.
2. **Anonymous.** 1994. 4-Vinylcyclohexene. IARC Monogr. Eval. Carcinog. Risks Hum. **60:**347–359.
3. **Borman, S. M., B. J. VanDePol, S. Kao, K. E. Thompson, I. G. Sipes, and P. B. Hoyer.** 1999. A single dose of the ovotoxicant 4-vinylcyclohexene diepoxide is protective in rat primary ovarian follicles. Toxicol. Appl. Pharmacol. **158:**244–252.
4. **Brunet, A., L. B. Sweeney, J. F. Sturgill, K. F. Chua, P. L. Greer, Y. Lin, H. Tran, S. E. Ross, R. Mostoslavsky, H. Y. Cohen, L. S. Hu, H. L. Cheng, M. P. Jedrychowski, S. P. Gygi, D. A. Sinclair, F. W. Alt, and M. E. Greenberg.** 2004. Stress-dependent regulation of FOXO transcription factors by the SIRT1 deacetylase. Science **303:**2011–2015.
5. **Castrillon, D. H., L. Miao, R. Kollipara, J. W. Horner, and R. A. DePinho.** 2003. Suppression of ovarian follicle activation in mice by the transcription factor Foxo3a. Science **301:**215–218.
6. **Chan, K., X. D. Han, and Y. W. Kan.** 2001. An important function of Nrf2 in combating oxidative stress: detoxification of acetaminophen. Proc. Natl. Acad. Sci. USA **98:**4611–4616.
7. **Chan, K., R. Lu, J. C. Chang, and Y. W. Kan.** 1996. NRF2, a member of the NFE2 family of transcription factors, is not essential for murine erythropoiesis, growth, and development. Proc. Natl. Acad. Sci. USA **93:**13943–13948.
8. **Chen, C. S., and K. R. Gee.** 2000. Redox-dependent trafficking of 2,3,4,5,6-pentafluorodihydrotetramethylrosamine, a novel fluorogenic indicator of cellular oxidative activity. Free Radic. Biol. Med. **28:**1266–1278.
9. **Devine, P. J., I. G. Sipes, M. K. Skinner, and P. B. Hoyer.** 2002. Characterization of a rat in vitro ovarian culture system to study the ovarian toxicant 4-vinylcyclohexene diepoxide. Toxicol. Appl. Pharmacol. **184:**107–115.
10. **Dinkova-Kostova, A. T., W. D. Holtzclaw, R. N. Cole, K. Itoh, N. Wakabayashi, Y. Katoh, M. Yamamoto, and P. Talalay.** 2002. Direct evidence that sulfhydryl groups of Keap1 are the sensors regulating induction of phase 2 enzymes that protect against carcinogens and oxidants. Proc. Natl. Acad. Sci. USA **99:**11908–11913.
11. **Elvin, J. A., and M. M. Matzuk.** 1998. Mouse models of ovarian failure. Rev. Reprod. **3:**183–195.
12. **Flaws, J. A., R. J. Sommer, E. K. Silbergeld, R. E. Peterson, and A. N. Hirshfield.** 1997. In utero and lactational exposure to 2,3,7,8-tetrachlorodibenzo-*p*-dioxin (TCDD) induces genital dysmorphogenesis in the female rat. Toxicol. Appl. Pharmacol. **147:**351–362.
13. **Gavrieli, Y., Y. Sherman, and S. A. Ben-Sasson.** 1992. Identification of programmed cell death in situ via specific labeling of nuclear DNA fragmentation. J. Cell Biol. **119:**493–501.
14. **Hirshfield, A. N.** 1991. Development of follicles in the mammalian ovary. Int. Rev. Cytol. **124:**43–101.
15. **Hoff, J.** 2000. Methods of blood collection in the mouse. Lab. Anim. **29:**47–53.
16. **Hosaka, T., W. H. Biggs III, D. Tieu, A. D. Boyer, N. M. Varki, W. K. Cavenee, and K. C. Arden.** 2004. Disruption of forkhead transcription factor (FOXO) family members in mice reveals their functional diversification. Proc. Natl. Acad. Sci. USA **101:**2975–2980.
17. **Hoyer, P. B., P. J. Devine, X. Hu, K. E. Thompson, and I. G. Sipes.** 2001. Ovarian toxicity of 4-vinylcyclohexene diepoxide: a mechanistic model. Toxicol. Pathol. **29:**91–99.

18. **Hoyer, P. B., and I. G. Sipes.** 1996. Assessment of follicle destruction in chemical-induced ovarian toxicity. Annu. Rev. Pharmacol. Toxicol. **36:**307–331.
19. **Hu, X., P. J. Christian, K. E. Thompson, I. G. Sipes, and P. B. Hoyer.** 2001. Apoptosis induced in rats by 4-vinylcyclohexene diepoxide is associated with activation of the caspase cascades. Biol. Reprod. **65:**87–93.
20. **Itoh, K., T. Chiba, S. Takahashi, T. Ishii, K. Igarashi, Y. Katoh, T. Oyake, N. Hayashi, K. Satoh, I. Hatayama, M. Yamamoto, and Y. Nabeshima.** 1997. An Nrf2/small Maf heterodimer mediates the induction of phase II detoxifying enzyme genes through antioxidant response elements. Biochem. Biophys. Res. Commun. **236:**313–322.
21. **Itoh, K., N. Wakabayashi, Y. Katoh, T. Ishii, K. Igarashi, J. D. Engel, and M. Yamamoto.** 1999. Keap1 represses nuclear activation of antioxidant responsive elements by Nrf2 through binding to the amino-terminal Neh2 domain. Genes Dev. **13:**76–86.
22. **Keller, D. A., S. C. Carpenter, S. Z. Cagen, and F. A. Reitman.** 1997. In vitro metabolism of 4-vinylcyclohexene in rat and mouse liver, lung, and ovary. Toxicol. Appl. Pharmacol. **144:**36–44.
23. **Kim, Y., K. Jung, T. Hwang, G. Jung, H. Kim, J. Park, J. Kim, D. Park, S. Park, K. Choi, and Y. Moon.** 1996. Hematopoietic and reproductive hazards of Korean electronic workers exposed to solvents containing 2-bromopropane. Scand. J. Work Environ. Health **22:**387–391.
24. **Kops, G. J., T. B. Dansen, P. E. Polderman, I. Saarloos, K. W. Wirtz, P. J. Coffer, T. T. Huang, J. L. Bos, R. H. Medema, and B. M. Burgering.** 2002. Forkhead transcription factor FOXO3a protects quiescent cells from oxidative stress. Nature **419:**316–321.
25. **Kwak, M. K., N. Wakabayashi, J. L. Greenlaw, M. Yamamoto, and T. W. Kensler.** 2003. Antioxidants enhance mammalian proteasome expression through the Keap1-Nrf2 signaling pathway. Mol. Cell. Biol. **23:**8786–8794.
26. **Leung, L., M. Kwong, S. Hou, C. Lee, and J. Y. Chan.** 2003. Deficiency of the Nrf1 and Nrf2 transcription factors results in early embryonic lethality and severe oxidative stress. J. Biol. Chem. **278:**48021–48029.
27. **Lu, A. Y., and G. T. Miwa.** 1980. Molecular properties and biological functions of microsomal epoxide hydrase. Annu. Rev. Pharmacol. Toxicol. **20:**513–531.
28. **Ma, Q.** 2004. Nrf2, an antioxidant activated CNC bZip transcription factor: mechanism of action and role in autoimmune function. Toxicologist **78:**252.
29. **Ma, Q., K. Kinneer, Y. Bi, J. Y. Chan, and Y. W. Kan.** 2004. Induction of murine NAD(P)H:quinone oxidoreductase by 2,3,7,8-tetrachlorodibenzo-*p*-dioxin requires the CNC (cap 'n collar) basic leucine zipper transcription factor Nrf2 (nuclear factor erythroid 2-related factor 2): cross-interaction between AhR (aryl hydrocarbon receptor) and Nrf2 signal transduction. Biochem. J. **377:**205–213.
30. **Ma, Q., and A. Y. Lu.** 2003. Origins of individual variability in P4501A induction. Chem. Res. Toxicol. **16:**249–260.
31. **Mattison, D. R.** 1980. Morphology of oocyte and follicle destruction by polycyclic aromatic hydrocarbons in mice. Toxicol. Appl. Pharmacol. **53:**249–259.
32. **Mattison, D. R., M. I. Evans, W. B. Schwimmer, B. J. White, B. Jensen, and J. D. Schulman.** 1984. Familial premature ovarian failure. Am. J. Hum. Genet. **36:**1341–1348.
33. **Mattison, D. R., B. S. Plowchalk, M. J. Meadows, M. M. Miller, A. Malek, and S. London.** 1989. The effect of smoking on oogenesis, fertilization, and implantation. Semin. Reprod. Endocrinol. **7:**291–304.
34. **Moi, P., K. Chan, I. Asunis, A. Cao, and Y. W. Kan.** 1994. Isolation of NF-E2-related factor 2 (Nrf2), a NF-E2-like basic leucine zipper transcriptional activator that binds to the tandem NF-E2/AP1 repeat of the beta-globin locus control region. Proc. Natl. Acad. Sci. USA **91:**9926–9930.
35. **Nemoto, S., and T. Finkel.** 2002. Redox regulation of forkhead proteins through a p66shc-dependent signaling pathway. Science **295:**2450–2452.
36. **Nguyen, T., C. S. Yang, and C. B. Pickett.** 2004. The pathways and molecular mechanisms regulating Nrf2 activation in response to chemical stress. Free Radic. Biol. Med. **37:**433–441.
37. **Ramos-Gomez, M., M. K. Kwak, P. M. Dolan, K. Itoh, M. Yamamoto, P. Talalay, and T. W. Kensler.** 2001. Sensitivity to carcinogenesis is increased and chemoprotective efficacy of enzyme inducers is lost in nrf2 transcription factor-deficient mice. Proc. Natl. Acad. Sci. USA **98:**3410–3415.
38. **Richards, J. S.** 1980. Maturation of ovarian follicles: actions and interactions of pituitary and ovarian hormones on follicular cell differentiation. Physiol. Rev. **60:**51–89.
39. **Smith, B. J., D. E. Carter, and I. G. Sipes.** 1990. Comparison of the disposition and in vitro metabolism of 4-vinylcyclohexene in the female mouse and rat. Toxicol. Appl. Pharmacol. **105:**364–371.
40. **Smith, B. J., D. R. Mattison, and I. G. Sipes.** 1990. The role of epoxidation in 4-vinylcyclohexene-induced ovarian toxicity. Toxicol. Appl. Pharmacol. **105:**372–381.
41. **Telford, W. G., A. Komoriya, and B. Z. Packard.** 2004. Multiparametric analysis of apoptosis by flow and image cytometry. Methods Mol. Biol **263:**141–160.
42. **Wang, L., D. Medan, R. Mercer, X. Shi, C. Huang, V. Castranova, M. Ding, and Y. Rojanasakul.** 2002. Role of neutrophil apoptosis in vanadium-induced pulmonary inflammation in mice. J. Environ. Pathol. Toxicol. Oncol. **21:**343–350.
43. **Whitlock, J. P., Jr.** 1999. Induction of cytochrome P4501A1. Annu. Rev. Pharmacol. Toxicol. **39:**103–125.
44. **Yoh, K., K. Itoh, A. Enomoto, A. Hirayama, N. Yamaguchi, M. Kobayashi, N. Morito, A. Koyama, M. Yamamoto, and S. Takahashi.** 2001. Nrf2-deficient female mice develop lupus-like autoimmune nephritis. Kidney Int. **60:**1343–1353.
45. **Yu, X., M. Kamijima, G. Ichihara, W. Li, J. Kitoh, Z. Xie, E. Shibata, N. Hisanaga, and Y. Takeuchi.** 1999. 2-Bromopropane causes ovarian dysfunction by damaging primordial follicles and their oocytes in female rats. Toxicol. Appl. Pharmacol. **159:**185–193.
46. **Zeidler, P. C., J. R. Roberts, V. Castranova, F. Chen, L. Butterworth, M. E. Andrew, V. A. Robinson, and D. W. Porter.** 2003. Response of alveolar macrophages from inducible nitric oxide synthase KO or Wt mice to an in vitro lipopolysaccharide or silica exposure. J. Toxicol. Environ. Health A **66:**995–1013.